Strategies for Synthesis of Elastomeric Polypropylene: Fluxional Metallocenes with C_1-Symmetry

Raisa Kravchenko,† Athar Masood,† Robert M. Waymouth,*,† and Charles L. Myers‡

Contribution from the Department of Chemistry, Stanford University, Stanford, California 94305, and Amoco Chemicals Development and Diversification, 150 West Warrenville Road, P. O. Box 3011, Naperville, Illinois 60566-7011

Received September 30, 1997

Abstract: The effects of replacing one of the 2-phenylindenyl-type ligands in bis(2-phenylindenyl)zirconium dichloride, $(2\text{-PhInd})_2ZrCl_2$ (**7**), a catalyst precursor for the production of elastomeric polypropylene (ELPP-7), with a cyclopentadienyl-type ligand have been studied. The mixed-ring compounds: (pentamethylcyclopentadienyl)(2-phenylindenyl)zirconium dichloride, Cp*(2-PhInd)$ZrCl_2$, (**8**), (pentamethylcyclopentadienyl)(1-methyl-2-phenylindenyl)zirconium dichloride, Cp*(1-Me-2-PhInd)$ZrCl_2$ (**9**), and (cyclopentadienyl)(2-phenylindenyl)zirconium dichloride, Cp(2-PhInd)$ZrCl_2$ (**10**), have been synthesized through the reaction of the corresponding lithium indenide with $C_5R_5ZrCl_3$ (**8** and **9**: R = CH_3; **10**: R = H). Crystal structures have been determined for complexes **8** and **9**. The behavior of the catalysts derived from complexes **8**, **9**, and **10** upon their activation by methylaluminoxane (MAO) for ethylene and propylene polymerization has been studied. Of all mixed-ring catalysts only **8**/MAO produces elastomeric polypropylene (ELPP-8) with properties consistent with a stereoblock microstructure. The stereosequence distributions in ELPP-8 determined from ^{13}C NMR spectra are very similar to those in elastomeric polypropylene generated with **7**/MAO under comparable conditions. However, the melting points and IR indices of **8**/MAO-derived samples are significantly lower than for samples of ELPP-7 with similar isotacticity which may be attributable to shorter isotactic block lengths in ELPP-8. At the same time, comparison of **8**/MAO to another metallocene system capable of producing elastomeric polypropylene *rac*-MeHC(Me_4Cp)(Ind)$TiCl_2$/MAO, **1**/MAO, described by Chien reveals significant similarities both in the catalyst symmetry and properties of generated polypropylene. The increase of isotacticity of ELPP-8 with propylene pressure similar to the trend observed for ELPP-7 favors the two-state mechanism of stereoblock formation with **8**/MAO.

Introduction

In the late 1950s, Natta discovered that one of the fractions of polypropylene produced by certain heterogeneous Ziegler−Natta catalysts had elastomeric properties.[1,2] Since the elastomeric component had partial crystallinity but could not be fractionated any further, Natta concluded that the polymer had a stereoblock microstructure in which amorphous and crystalline segments were parts of the same polypropylene chain. Several research groups attempted to develop improved catalysts for the synthesis of polypropylene elastomers (ELPP), but their success was limited by low catalyst productivities and low content of elastomeric material in the resulting product.[3−5] Two decades after Natta's initial discovery, Collette and co-workers at DuPont reported the development of improved heterogeneous catalysts for the production of elastomeric polypropylene which did not need to be fractionated to be a useful elastomer.[6,7]

The first homogeneous catalyst that generated elastomeric polypropylene (ELPP-1), C_1-symmetric bridged titanocene **1** (Scheme 1), was described by Chien and co-workers.[8−10] Homogeneous tacticity and length distributions among different polymer chains, suggested by complete solubility in ether and narrow molecular weight distributions (MWD) of ELPP-1, were in agreement with the presence of a single type of active species.[8,10] To account for the formation of a stereoblock microstructure Chien proposed a two-state mechanism, similar to that originally proposed by Coleman and Fox for anionic polymerization of acrylates.[11] Chien hypothesized that monomer insertion occurred sequentially at aspecific and isospecific coordination sites of the catalyst (Scheme 1). To clarify the mechanism of stereoblock formation with titanocene **1**, Gauthier and Collins prepared a number of structurally related catalysts (**2**−**6**, Scheme 1) and investigated their polymerization behavior.[12,13] Only the hafnocene derivatives **4** and **6,** capable of

* Corresponding author: Phone: 650 723 4515. E-mail: waymouth@leland.stanford.edu.

† Stanford University.

‡ Amoco Chemicals Development and Diversification.

(1) Natta, G.; Mazzanti, G.; Crespi, G.; Moraglio, G. *G. Chim. Ind.* **1957**, *39*, 275−283.

(2) Natta, G. *J. Polym. Sci.* **1959**, *34*, 531−549.

(3) Schrage, A. (Rexall) U.S. Patent 3,329, 741, **1967**.

(4) Gobran, R. (3M) U.S. Patent 3,784, 502, **1974**.

(5) Kontos (US Rubber) U.S. Patent 3,853, 969, **1974**.

(6) Collette, J. W.; Tullock, C. W.; MacDonald, R. N.; Buck, W. H.; Su, A. C. L.; Harrel, J. R.; Mulhaupt, R.; Anderson, B. C. *Macromolecules* **1989**, *22*, 3851−3858.

(7) Collette, J. W.; Ovenall, D. W.; Buck, W. H.; Ferguson, R. C. *Macromolecules* **1989**, *22*, 3858−3866.

(8) Mallin, D. T.; Rausch, M. D.; Lin, Y. G.; Dong, S.; Chien, J. C. W. *J. Am. Chem. Soc.* **1990**, *112*, 2030−2031.

(9) Chien, J. C. W.; Llinas, G. H.; Rausch, M. D.; Lin, G. Y.; Winter, H. H.; Atwood, J. L.; Bott, S. G. *J. Am. Chem. Soc.* **1991**, *113*, 8569−8570.

(10) Llinas, G. H.; Dong, S. H.; Mallin, D. T.; Rausch, M. D.; Lin, Y. G.; Winter, H. H.; Chien, J. C. W. *Macromolecules* **1992**, *25*, 1242−1253.

(11) Coleman, B. D.; Fox, T. G. *J. Chem. Phys.* **1963**, *38*, 1065−1075.

(12) Gauthier, W. J.; Corrigan, J. F.; Taylor, N. J.; Collins, S. *Macromolecules* **1995**, *28*, 3771−3778.

S0002-7863(97)03414-8 CCC: $15.00
Published on Web 02/20/1998

Scheme 1. Bridged Metallocenes for the Production of Elastomeric Polypropylene

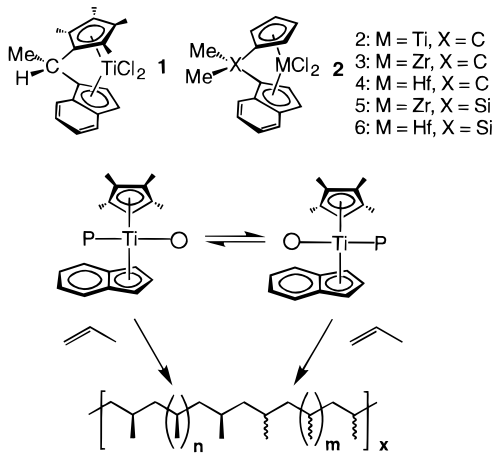

Scheme 2. Unbridged 2-Arylindene Catalysts for the Production of Elastomeric Polypropylene

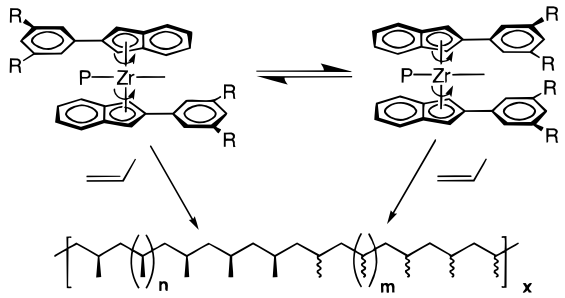

polymerizing propylene to high molecular weight, produced elastomeric polypropylene (ELPP-4 and -6).[12] The microstructure of these polymers, determined by ^{13}C NMR spectroscopy, was simulated using statistical models based on different mechanisms for monomer insertion on the two inequivalent coordination sites of the catalyst.[13] The microstructure could be described equally well by two models: the "two-state" consecutive model proposed by Chien and a "random" model, in which insertions took place competitively on both coordination sites. The average isotactic block length predicted by both models was approximately 10 propylene units,[13] which was in agreement with the low melting points observed for ELPP-1, -4, and -6.[8,10,12]

Recently we reported a strategy for the production of stereoblock polypropylene with a nonbridged metallocene, bis-(2-phenylindenyl)zirconium dichloride, $(2\text{-PhInd})_2ZrCl_2$ (**7**).[14] The catalyst was designed to switch its coordination geometry from aspecific to isospecific during the course of polymerization in order to generate atactic and isotactic blocks (Scheme 2). Since it was known that bis(indenyl)zirconocene catalyst produced atactic polypropylene,[15] 2-phenyl substituents were introduced in catalyst **7** to slow the ligand rotation and allow insertion of several monomer units before the rotamers interconverted. Polypropylene produced with **7**/MAO (ELPP-7) could be fractionated into ether soluble, heptane soluble, and heptane insoluble fractions with similar molecular weights.[14,16,17]

Scheme 3. Mixed Ring Catalysts

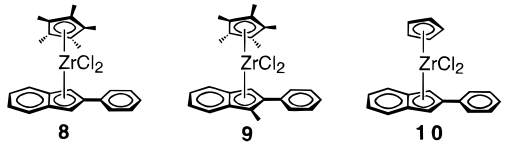

Scheme 4. Synthesis of Mixed-Ring Metallocenes

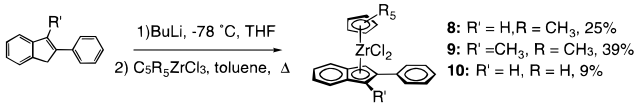

The fractionation results implied that the polymer was characterized by a distribution of atactic and isotactic block lengths. Melting temperatures of 140−150 °C suggested the presence of long crystallizable sequences. In agreement with the "two-state" model, the isotactic pentad content in polypropylene generated with **7**/MAO increased with propylene pressure.[11,14,18,19] The isospecificity of the catalyst could be influenced by the substitution on the phenyl rings which in combination with the stereospecificity control by propylene pressure variation allowed us to synthesize materials ranging in properties from excellent elastomers to tough plastics.[18,20]

To better understand the structural features required for the production of a stereoblock microstructure, we have prepared mixed-ring complexes **8**−**10** (Scheme 3) in which one of the 2-phenylidenyl-type ligands has been replaced with a pentamethylcyclopentadienyl (**8**, **9**) or a cyclopentadienyl ligand (**10**). The polymerization behavior of the modified catalysts **8**−**10**/MAO is compared to that of catalysts **7**/MAO and **1**/MAO to investigate the role of torsional isomerism.[21−24]

Experimental Section

General Considerations. All organometallic reactions were conducted using standard Schlenk and drybox techniques. Elemental analyses were conducted by Desert Analytics. Unless otherwise specified all reagents were purchased from commercial suppliers and used without further purification. Bis-(2-phenylindenyl)zirconium dichloride (**7**) and 1-methyl-2-phenylindene were prepared according to the literature procedures.[14,18,20,25] Hexane, pentane, and methylene chloride used in organometallic synthesis were distilled from calcium hydride under nitrogen. Tetrahydrofuran was distilled from sodium/benzophenone under nitrogen. Toluene was passed through two purification columns packed with activated alumina and supported copper catalyst.[26] Chloroform-d_3 and methylene chloride-d_2 were distilled from calcium hydride.

(Pentamethylcyclopentadienyl)(2-phenylindenyl)zirconium Dichloride (8). Butyllithium (2.0 M in pentane, 3.9 mL, 7.8 mmol) was added dropwise to a suspension of 2-phenylindene (1.441 g, 7.5 mmol) in THF (30 mL) at −78 °C. As the deprotonation of 2-phenylindene

(13) Gauthier, W. J.; Collins, S. *Macromolecules* **1995**, *28*, 3779−3786.
(14) Coates, G. W.; Waymouth, R. M. *Science* **1995**, *267*, 217−219.
(15) Resconi, L.; Abis, L.; Franciscono, G. *Macromolecules* **1992**, *25*, 6814−6817.
(16) Resconi, L.; Piemontesi, F.; Yu, L.-C. (Montell) PCT Int. Appl. 9620225 A2, **1996**.
(17) Carlson, E. D.; Terakawa, T.; Fuller, G. G.; Krejchi, M. T.; Shah, C.; Waymouth, R. M. **1997**, submitted for publication.
(18) Hauptman, E.; Waymouth, R. M.; Ziller, J. W. *J. Am. Chem. Soc.* **1995**, *117*, 11586−11587.
(19) Bruce, M. D.; Coates, G. W.; Hauptman, E.; Waymouth, R. M.; Ziller, J. W. *J. Am. Chem. Soc.* **1997**, *119*, 11174−11182.
(20) Waymouth, R. M.; Coates, G., W.; Hauptman, E. (Stanford University) U.S. Patent 5,594, 080, **1997**.
(21) Knickmeier, M.; Erker, G.; Fox, T. *J. Am. Chem. Soc.* **1996**, *118*, 9623−9630.
(22) Erker, G.; Aulbach, M.; Knickmeier, M.; Wingbermuhle, D.; Kruger, C.; Nolte, M.; Werner, S. *J. Am. Chem. Soc.* **1993**, *115*, 4590−4601.
(23) Kruger, C.; Lutz, F.; Nolte, M.; Erker, G.; Aulbach, M. *J. Organomet. Chem.* **1993**, *452*, 79−86.
(24) Kruger, C.; Nolte, M.; Erker, G.; Thiele, S. *Z. Naturforsch* **1992**, *47b*, 995−999.
(25) Kravchenko, R. L.; Masood, A.; Waymouth, R. M. *Organometallics* **1997**, *16*, 3635−3639.
(26) Pangborn, A. B.; Giardello, M. A.; Grubbs, R. H.; Rosen, R. K.; Timmers, F. J. *Organometallics* **1996**, *15*, 1518−1520.

occurred, the mixture became homogeneous to give dark orange solution of lithium 2-phenylindenide. When the addition of the reagents was complete, the solution was gradually warmed to room temperature, stirred for 30 min, and then evaporated to dryness. The resulting yellow solid was combined with Cp*$ZrCl_3$ (2.500 g, 7.5 mmol) and toluene (40 mL). The mixture was heated to 70 °C and stirred for 36 h. The turbid yellow solution was filtered through a glass frit packed with Celite. The Celite layer was washed with toluene (3 × 10 mL). The combined filtrates were evaporated to dryness. The solid (3.078 g, 79% crude yield) was dissolved in CH_2Cl_2 (15 mL), and the resulting solution was carefully layered with pentane (40 mL). The layered solution was placed in a −18 °C freezer, and light yellow crystals formed after 5 days (0.974 g, 25% yield). ^{1}H NMR ($CDCl_3$, 20 °C, 300 MHz): δ 7.78 (d, J = 7.1 Hz, 2H), 7.52 (dd, J = 6.4 Hz, J = 3.2 Hz, 2H), 7.44 (t, J = 7.2 Hz, 2H), 7.35 (t, J = 7.3 Hz, 1H), 7.22 (dd, J = 6.5 Hz, J = 3.1 Hz, 2H), 6.87 (s, 2H), 1.84 (s, 15 H). ^{13}C {^{1}H} NMR[27] ($CDCl_3$, 20 °C, 75 MHz): δ 132.61 (C), 131.84 (C), 128.41 (CH), 128.37 (CH), 128.12 (CH), 127.19 (C), 126.22 (CH), 124.99 (C), 124.32 (CH), 103.64 (CH), 12.34 (CH_3). Anal. Found (Calcd): C, 61.27 (61.45); H, 5.31 (5.36).

(Pentamethylcyclopentadienyl)(1-methyl-2-phenylindenyl)zirconium Dichloride (9). Butyllithium (2.5 M in hexanes, 3.8 mL, 9.5 mmol) was added dropwise to the solution of 1-methyl-2-phenylindene (1.860 g, 9.0 mmol) in THF (20 mL) at −78 °C. When the addition was complete, the dark yellow solution was slowly warmed to room temperature, stirred for 30 min, and then evaporated to dryness. The resulting dark yellow solid was combined with Cp*$ZrCl_3$ (3.0 g, 9.0 mmol) and toluene (50 mL). The mixture was heated to 70 °C and stirred for 12 h. The resulting turbid yellow solution was cooled to room temperature and filtered through a glass frit packed with Celite. The Celite layer was washed with toluene (5 × 25 mL). The combined filtrates were concentrated to a volume of 20 mL, and a yellow powdery solid precipitated out of the solution. The mother liquor was decanted, and the product dried in *vacuo* (1.500 g, 38%). Yellow rodlike crystals suitable for X-ray analysis were obtained from a THF/pentane solution at −18 °C. ^{1}H NMR ($CDCl_3$, 20 °C, 300 MHz): δ 7.50 (t, J = 6.84, 2H), 7.33 (m, 6H), 7.04 (t, J = 7.6 Hz, 1H), 6.46 (s, 1H), 2.54 (s, 3H), 1.79 (s, 15H). ^{13}C {^{1}H} NMR[27] ($CDCl_3$, 20 °C, 75 MHz): δ 133.06 (C), 131.49 (C), 130.85 (C), 130.14 (CH), 128.32 (CH), 127.94 (CH), 126.29 (CH), 126.03 (CH), 124.39 (CH+C), 122.82 (C), 122.61 (CH), 121.99 (C), 95.49 (CH), 12.27 (CH_3, Cp*), 11.86 (CH_3). Anal. Found (Calcd): C, 62.13 (62.13); H, 5.80 (5.61)

(Cyclopentadienyl)(2-phenylindenyl)zirconium Dichloride (10). Butyllithium (2.5 M in hexane, 4.4 mL, 11 mmol) was added dropwise to a suspension of 2-phenylindene (2.022 g, 11 mmol) in THF (40 mL) at −78 °C. The resulting orange homogeneous mixture was gradually warmed to room temperature, stirred for 60 min, and then evaporated to dryness. The resulting orange solid was combined with $CpZrCl_3$ (2.763 g, 11 mmol) and toluene (70 mL). The reaction mixture was stirred at 30 °C for 24 h. The turbid yellow solution was filtered through a glass frit packed with Celite to give a brown solution. The Celite layer was washed with toluene (20 mL). The combined filtrates were evaporated to dryness. An ^{1}H NMR spectroscopic analysis showed that the resulting green-yellow solid contained a mixture of **10** and **7**. Repeated crystallization from a concentrated toluene solution at −18 °C afforded pure **10** (0.420 mg, 9% yield). ^{1}H NMR (20 °C, $CDCl_3$, 300 MHz): δ 7.71 (d, J = 7.2 Hz, 2H), 7.64 (dd, J = 6.5 Hz, J = 3.0 Hz, 2H), 7.49 (t, J = 7.3 Hz, 2H), 7.38 (t, J = 7.2 Hz, 1H), 7.30 (dd, J = 6.5 Hz, J = 3.0 Hz, 2H), 6.92 (s, 2H), 6.10 (s, 5H). ^{13}C {^{1}H} NMR[27] ($CDCl_3$, 20 °C, 75 MHz): δ 134.8 (C), 133.3 (C), 129.0 (CH), 128.9 (CH), 127.2 (C), 126.7 (CH), 126.4 (CH), 125.1 (CH), 116.7 (CH), 100.9 (CH). Anal. Found (Calcd): C, 57.16 (57.40), H, 3.67 (3.85).

X-ray Structure Determination of 8. A single crystal of complex **8** was mounted in paratone oil on a glass fiber and placed in a cold stream of nitrogen on an Enraf-Nonius CAD4 diffractometer with graphite monochromated Mo K_α radiation. Cell constants and an orientation matrix for data collection obtained from a least-squares refinement using the setting angles of 25 centered reflections (22 in the range $35 < 2\theta < 36°$ and 3 in the range $20 < 2\theta < 21°$) corresponded to a primitive triclinic cell with dimensions: a = 9.638(2) Å, b = 9.522(1) Å, c = 12.100(2) Å, α = 88.06(1)°, β = 86.26(2)°, γ = 75.56(1)°. The data were collected at −75 °C using the ω scan technique to a maximum 2θ value of 50°.

A total of 4007 reflections were collected of which 3062 were unique. Over the course of data collection, the intensity standard decreased by an average of 0.1%. No decay correction was applied.

The structure was solved by direct methods and expanded using Fourier techniques. All non-hydrogen atoms were refined anisotropically. Hydrogen atoms were located by difference Fourier maps but included initially at idealized positions 0.95 Å from their parent atoms before the last cycle of refinement. The final cycle of full-matrix least-squares refinement was based on 3698 observed reflections and 254 variable parameters and converged with R (R_w) = 3.0 (4.0).

X-ray Structure Determination of 9. The crystal mounting procedure and conversion of the raw intensity data were the same as above. The complex was found to crystallize in a primitive monoclinic cell with dimensions: a = 9.196(1) Å, b = 24.362(1) Å, c = 10.303(1) Å, α = 89.980(5)°, β = 100.237(4)°, γ = 90.005(5)°. Over the course of the data collection the intensity standards decreased by an average of 0.2%. No decay correction was applied.

The structure was solved by the methods described above. In a late stage of the refinement it became apparent that the carbon atoms of the pentamethylcyclopentadienyl moiety were disordered, and these atoms were treated as two rigid groups with occupancy of 0.6 and 0.4, respectively, and refined isotropically; hydrogen atoms associated with these groups were not included into the refinement. The final cycle of full-matrix least squares refinement was based on 2842 observed reflections and 186 variable parameters and converged with R (R_w) = 6.8 (7.5).

Tables of the anisotropic thermal coefficients, bond lengths, bond angles, torsion angles, and H-atom coordinates for complexes **8** and **9** are available as Supporting Information.

Ethylene and Propylene Polymerizations. Polymerization grade ethylene and propylene gases were purchased from Matheson, and liquid propylene was obtained from Amoco. Both monomers were further purified by passage through two columns packed with activated alumina and supported copper catalyst. Methylaluminoxane (MAO), type 3A, purchased from Akzo, was dried *in vacuo* prior to use.

Polymerizations in Toluene Solution. A 300-mL stainless steel Parr reactor equipped with a mechanical stirrer was charged with dry methylaluminoxane and toluene (80 mL). A 50-mL pressure tube was charged with the solution of the zirconocene in toluene (20 mL). The reactor was purged with the corresponding monomer 3−4 times by pressurizing and venting. The mixture was allowed to equilibrate for 30 min at the polymerization temperature and pressure with constant stirring. The pressure tube with the metallocene solution was pressurized to 200 psig with argon, and the solution was injected into the reactor. After a certain time the reaction was quenched by injecting methanol (20 mL). Polypropylene was precipitated by pouring its toluene solution into acidified MeOH (5% HCl), filtered, washed with MeOH, and dried in a vacuum oven at 40 °C to constant weight. Polyethylene was collected by filtration and dried in a vacuum oven at 40 °C to constant weight.

Polymerizations in Liquid Propylene. A 300- or 450-mL stainless steel Parr reactor equipped with a mechanical stirrer was evacuated, purged 4−5 times with gaseous propylene by pressurizing and venting, and charged with liquid propylene (100 mL in the case of 300-mL Parr and 230 mL in the case of 450-mL Parr reactor). The monomer was equilibrated at the reaction temperature, and the reaction was initiated by injecting the zirconocene/MAO solution in toluene (20 mL) under Ar pressure (250 psig × 30 mL). After a certain time the reaction was quenched by injecting MeOH (20 mL). The polymer was precipitated in acidified MeOH (5% HCl), filtered, washed with methanol, and dried in a vacuum oven at 40 °C to constant weight.

Polymer Characterization. Polymer molecular weights and molecular weight distributions were determined by high-temperature gel permeation chromatography using polypropylene and polyethylene as GPC calibration standards. ^{13}C NMR measurements were performed

(27) Primary, secondary, and tertiary carbon atoms were assigned based on APT experiments.

Table 1. Selected Dihedral Angles and Bond Lengths for Complexes 7-9.

	dihedral angle (deg)		bond distance (Å)	
complex	plane 1/ plane 2[a]	plane 3/ plane 4[b]	C(2)−C(10)	C(17)−C(25)
8	12.5(4)		1.479(3)	
9	42(1)		1.48(1)	
7-anti[14]	11.54	13.53	1.476(5)	1.472(6)
7-syn[14]	10.44	12.72	1.468(7)	1.485(5)

[a] Plane 1 = C(1)−C(9), plane 2 = C(10)−C(15). [b] Plane 3 = C(16)−C(24), plane 4 = C(25)−C(30).

Table 2. Ethylene Polymerization with Complexes **7**−**10**/MAO[a]

entry	catalyst	productivity[b]	Mw·10^{-3} [c]	MWD[c]
1	**7**/MAO	3570	2040	3.2
2	**8**/MAO	3470	1883	4.0
3	**9**/MAO	4810	1982	3.9
4	**10**/MAO	10450	863	3.1

[a] Reaction conditions: P_E = 25 psig, [Zr] = 5 × 10^{-6} M, t_{rxn} = 1 h, T = 20 ± 1 °C, [Zr]:[MAO] = 1:2750. [b] kg·PE/mol·Zr·h. [c] Determined by high-temperature GPC.

Table 3. Propylene Polymerization with Catalysts **7**−**10**/MAO[a]

entry	catalyst	productivity[b]	% *m*[c]	% *mmmm*[c]	Mw·10^{-3} [d]	MWD[d]
1	**7**/MAO[18]	1700	70	33	369	3.9
2	**8**/MAO	490	70	30	100	6.8
3	**9**/MAO	25	58	17[e]	21.6	8.9
4	**10**/MAO	5900	55	8	113	2.1

[a] T = 20 ± 1 °C, [Zr]:[MAO] = 1000, t_{rxn} = 1 h, P_p = 75 psig, [Zr] = 5 × 10^{-5} M. [b] kg·PP/mol·Zr·h. [c] Determined by ^{13}C NMR spectroscopy. [d] Determined by high temperature GPC. [e] Error may be present due to the overlap with chain-end signals.[34,35]

on Varian XL 400 and Varian UI 300 instruments at 100 °C in 1,1,2,2-tetrachloroethane-d_2 using an acquisition time of 1 s with no additional delays between pulses. All spectra were referenced to the solvent resonance. It was assumed that the relaxation times and NOEs of all methyl groups were the same.[28−32] The areas of the nine peaks in the methyl region determined from spectral integrations were used to characterize the sample microstructure. Melting points and heats of fusion were determined by differential scanning calorimetry using Perkin-Elmer DSC-7. The DSC scans were obtained by first heating polypropylene samples prepared with **7** and **8**/MAO to 180 and 120 °C, respectively, for 20 min, cooling them to 20 °C over 2 h, aging them at room temperature for 16 h, and then reheating them from 20 °C to 200 °C at 20 °C/min. All DSC values in the tables are reheat values. Infrared spectra were obtained by transmission on melt-pressed films using a Perkin-Elmer 1600 FTIR spectrometer. The IR ratio = A_{993}/A_{975}, calculated from the absorptivities at 993 and 975 cm^{-1},[33] was averaged over at least three measurements taken in different regions of the film.

Mechanical property tests of ELPP-8 were conducted with ASTM D1708 dumbbell specimens (2 cm × 0.5 cm gauge) which were die cut from compression molded plaques (0.13 cm thickness). Plaques (15.2 cm diameter) were compression molded with a mold cavity temperature of 90 °C for sample RK-6-80 (M_w = 124 000, entry 6 in Table 4) and 160 °C for sample RK-6-24 (M_w = 455 000, entry 5 in Table 4), with mold pressure incrementally increased to 6 tons as the polymer melted. Plaques were demolded after cooling to 23 °C and conditioned for at least 3 days. Tensile and recovery methods were adopted from Collette et al.[6] Crosshead separation rate was 51 cm/min. Recovery/set tests were conducted by elongating the specimen to 300% and immediately reversing at the same rate to zero stress. % Set represents the % increase in specimen gauge length upon recovery. % Recovery values represent the fraction of the elongation which is restored during recovery, × 100. Hysteresis tests were run with consecutive 300%, 500%, 700% elongation and recovery cycles and an elongation to break. The ELPP-7 sample 11784-133-1, for general mechanical property comparison to ELPP-8, was a larger scale (8 L reactor) bulk propylene polymerization. Several closely similar batches were combined, stabilized, pelletized, and extruded (190 °C) into 11 cm wide, 0.04 cm thick unoriented sheet. Specimen type (ASTM D1708) and test methods were the same as for ELPP-8.

Table 4. Dependence of Propylene Polymerization Productivity of Cp*(2-PhInd)$ZrCl_2$ 8/MAO on Polymerization Time and Temperature[a]

entry	t_p, min	T, °C	productivity[b]	% *mmmm*[c]	Mw·10^{-3} [d]	MWD[d]
1	35	20	780	36	127	3.5
2	160	20	380	36	128[e]	3.8[e]
3	195	20	310	36		
4	52	4	1900	42	597	4.5
5	150	5	890	40	455	4.8
6[f]	210	10	700	39	124	3.2

[a] Reaction conditions: [Zr]:[MAO] = 1000, [Zr] = 5 × 10^{-5} M, bulk propylene. [b] kg·PP/mol·Zr·h. [c] Determined by ^{13}C NMR. [d] Determined by high temperature GPC. [e] Combined samples 2 and 3. [f] MAO type 4 from Akzo was used which contains more of trimethylaluminum than type 3A.

Polypropylene Extraction. The extraction of a polypropylene sample obtained with **8**/MAO (entry 5 in Table 5) with boiling ether was conducted in a Soxhlet extractor under argon for 24 h. The soluble polymer was precipitated in acidified methanol, filtered, and dried in a vacuum oven at 40 °C overnight.

Results

Zirconocene Synthesis and Structure. Mixed-ring zirconocene complexes **8**, **9**, and **10** were prepared from the corresponding lithium indenide and $C_5R_5ZrCl_3$ (R = CH_3 for **8** and **9,** and R = H for **10**) in toluene (Scheme 3). This route gave zirconocenes **8** and **9** in satisfactory yields (25 and 39%, respectively). The major loss in the yield for **8** occurred at the recrystallization step: due to the high solubility of this complex in most solvents only a small amount of it crystallized even under optimized conditions. In contrast, complex **9** was much less soluble in common solvents than **8** which simplified its isolation. The chosen synthetic route did not work very well for complex **10**: a significant amount of complex **7** (2-PhInd)$_2ZrCl_2$ formed during the synthesis possibly due to the contamination of $CpZrCl_3$ with $ZrCl_4$. Lower solubility of **7** in toluene allowed to remove it almost completely as the first recrystallization crop and isolate **10** in subsequent crystallization but only in a 9% yield.

At room-temperature complexes **8** and **10** were characterized by only one ^{1}H NMR signal for the cyclopentadienyl protons of 2-phenylindenyl (δ = 6.87 and 6.92 ppm, respectively), and only one methyl proton signal was observed for complex **9** (δ = 2.54 ppm) which suggested fast ligand rotation on the NMR time scale. For complex **8** the ligand rotation could not be frozen even at temperatures as low as −80 °C: the signals of the Cp* methyls and cyclopentadienyl protons broadened but did not split.

The crystal structures of complexes **8** (Figure 1) and **9** (Figure 2) were determined by X-ray diffraction. The metal-centroid bond angles in **8** (133.8°) and **9** (132.6°) were slightly larger

(28) Vizzini, J. C.; Chien, J. C. W.; Babu, G. N.; Newmark, R. A. *J. Polym. Sci.: Part A: Polym. Chem.* **1994**, *32*, 2049−2056.
(29) Segre, A. L.; Andruzzi, F.; Lupinacci, D.; Magagnini, P. L. *Macromolecules* **1983**, *16*, 1207−1212.
(30) Inoue, Y.; Nishioka, A.; Chujo, R. *Makromol. Chem.* **1973**, *168*, 163−172.
(31) Randall, J. C. *J. Polym. Sci., Polym. Phys. Ed.* **1976**, *14*, 1693−1700.
(32) Schilling, F. C. *Macromolecules* **1978**, *11*, 1290−1291.
(33) Luongo, J. P. *J. Appl. Polym. Sci.* **1960**, *3*, 302.

Table 5. Propylene Polymerization with (2-PhInd)$_2$ZrCl$_2$ 7/MAO and Cp*(2-PhInd)ZrCl$_2$ 8/MAO under Various Conditions

entry	catalyst	$P_{p,\ psig}$	T, °C	productivity[a]	% *m*[b]	% *mmmm*[b]	IR ratio[c]	Mw·10^{-3} [d]	MWD[d]	T_m range,[e] °C	ΔH_m,[e] J/g
1	**8**/MAO	25	20	170	67	21	n.d.	62.7	4.7	n.d.	n.d.
2	**8**/MAO	50	20	360	70	28	0.22	84.7	4.8	29−63	1.0
3	**8**/MAO	75	20	490	70	30	0.24	100	6.8	34−69	4.9
4	**8**/MAO	100	20	560	74	34	0.28	122	3.7	34−74	8.6
5	**8**/MAO	bulk	20	780	74	36	0.32	127	3.5	29−87	13.6
6	**8**/MAO	bulk	4	1900	78	42	0.35	597	4.5	30−103	16.2
7	**7**/MAO	50	25	880	66	26	0.27	241	3.5	30−149	22.3
8	**7**/MAO	90	25	2400	73	32	0.36	369	3.9	30−155	27.4
9	**7**/MAO	bulk	20	3030	70	33	0.38	542	3.5	30−152	28.0

[a] kg·PP/mol·Zr·h. [b] Determined from ^{13}C NMR spectroscopy. [c] IR ratio = A_{993}/A_{975}, calculated from the absorptivities at 993 and 975 cm^{-1}.[33] [d] Determined by high temperature GPC. [e] Determined by DSC.

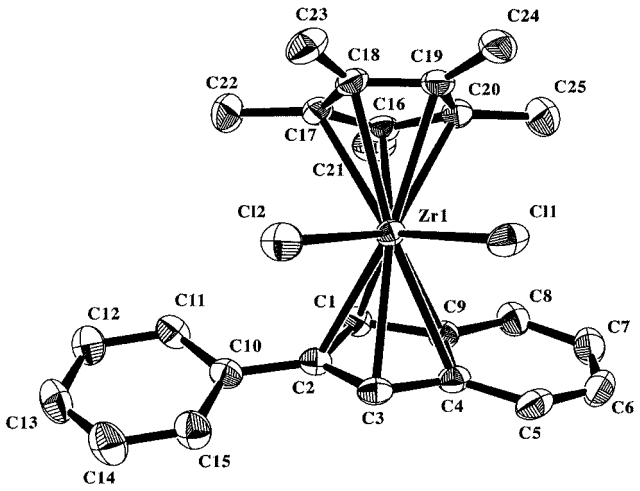

Figure 1. X-ray crystal structure of complex **8**, showing atom-labeling scheme.

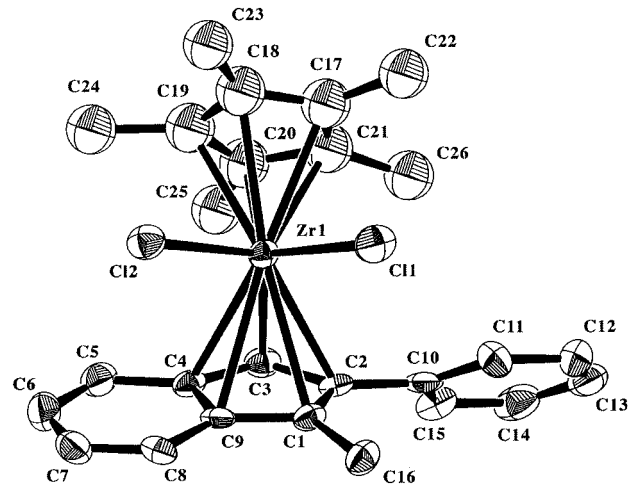

Figure 2. X-ray crystal structure of complex **9**, showing atom-labeling scheme.

than those for (2-PhInd)$_2$ZrCl$_2$ (131°).[14] Substitution of the 2-phenylindenyl ligand with a methyl group in position 1 resulted in an increase of the dihedral angle between the phenyl and the indenyl rings: in Cp*(1-Me-2-PhInd)ZrCl$_2$ **9** this angle was significantly larger (42°) than in (2-PhInd)$_2$ZrCl$_2$ **7** and Cp*-(2-PhInd)ZrCl$_2$ **8** (10−12°) (Table 1).[25]

Ethylene Polymerization. Ethylene polymerization results for catalysts **7**−**10**/MAO are summarized in Table 2. Polymerization productivities and polyethylene molecular weights observed for Cp*(2-PhInd)ZrCl$_2$ **8**/MAO and Cp*(1-Me-2-PhInd)ZrCl$_2$ **9**/MAO were similar to those observed for (2-PhInd)$_2$ZrCl$_2$ **7**/MAO. Catalyst Cp(2-PhInd)ZrCl$_2$ **10**/MAO was more productive but gave polyethylene of lower molecular weight than **7**/MAO.

Propylene Polymerization. Table 3 summarizes the results of propylene polymerization with **7**−**10**/MAO. At 20 °C and 75 psig of propylene the polymerization productivity and polypropylene molecular weight observed for Cp*(2-PhInd)-ZrCl$_2$ **8**/MAO were approximately 1/3 of those observed for (2-PhInd)$_2$ZrCl$_2$ **7**/MAO. Catalyst Cp*(1-Me-2-PhInd)ZrCl$_2$ **9**/MAO was essentially inactive for propylene polymerization and generated milligram quantities of low molecular weight material in hour-long polymerization runs. As observed for ethylene polymerization, Cp(2-PhInd)ZrCl$_2$ **10**/MAO had higher productivity than **7**/MAO but gave polymer of a lower molecular weight. The molecular weight distributions observed for polypropylene generated by **8** and **9**/MAO under these conditions were broader than for the polymer generated by **7**/MAO. Catalyst **10**/MAO gave polypropylene with the narrowest MWD of all four catalysts.

Polypropylene generated with **10**/MAO was amorphous and essentially atactic (% *mmmm* = 8). A higher isotactic pentad content was observed for polypropylene produced by **9**/MAO (% *mmmm* = 17), but the extremely low productivity of this catalyst precluded any further studies of its stereospecificity. The isotactic pentad content and microstructure of polypropylene generated with **8**/MAO (% *mmmm* = 30) were essentially the same as those observed for polypropylene generated with **7**/MAO (% *mmmm* = 33) under similar conditions (see Supporting Information for listings of pentad distribution for representative samples). Furthermore, the polymer generated by Cp*(2-PhInd)ZrCl$_2$ **8**/MAO was also elastomeric (ELPP-8), which prompted us to investigate the polymerization behavior of this catalyst in more detail.

The results of propylene polymerizations conducted with catalyst **8**/MAO under various conditions and selected characteristics of the polymers are summarized in Tables 4 and 5. Propylene polymerization data for (2-PhInd)$_2$ZrCl$_2$ **7**/MAO are given in Table 5 for comparison. Both at 20 °C (entries 1−3, Table 4) and 4−5 °C (entries 4 and 5, Table 4), the polymerization productivity of **8**/MAO dropped with increasing polymerization time suggesting that the catalyst was gradually deactivated. The isotactic pentad content, molecular weights, and molecular weight distributions of polypropylene generated by **8**/MAO did not appear to be dependent on polymerization time. The productivity and stereospecificity of **8**/MAO in bulk propylene were higher at 5 °C than at 20 °C (Table 4). Higher productivity of **8**/MAO at lower temperature indicated higher stability of the catalytically active centers under these conditions. Similarly to (2-PhInd)$_2$ZrCl$_2$ **7**/MAO, at 20 °C the polymerization productivity of **8**/MAO increased with increasing propylene pressure (Table 5). The isotactic pentad content in polypropylene generated with **8**/MAO also increased with

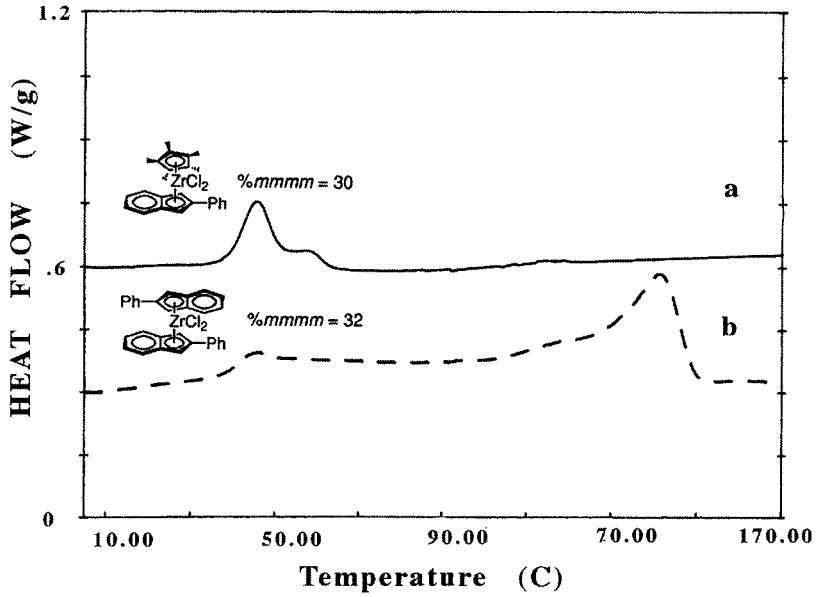

Figure 3. Melting curves for polypropylene generated with Cp*(2-PhInd)$ZrCl_2$ **8**/MAO (a), for sample description see entry 3 in Table 5, and (2-PhInd)$_2ZrCl_2$ **7**/MAO (b), for sample description see entry 8 in Table 5, determined by differential scanning calorimetry.

Table 6. Mechanical Properties of Cp*(2-PhInd)$ZrCl_2$ 8/MAO-Derived Elastomeric Polypropylene (ELPP-8) in Comparison to Other ELPP Polymers

ELPP type catalyst	ELPP-1[a] Chien's catalyst[10]		ELPP-7 [b] (2-PhInd)$_2ZrCl_2$ **7**/MAO	ELPP-8 Cp*(2-PhInd)ZrCl2 8/MAO	
				c	*d*
$M_n \cdot 10^{-3}$ [e]	66	98	84 (ave)	39	95
$M_w \cdot 10^{-3}$ [e]	127	164	254 (ave)	124	455
melting peaks, °C[f]	51, 66	53, 64	49, 148	39, 68	46, 79
% *mmmm*[g]	40	n/a	36 (ave)	39	40
density	n/a	n/a	n/a	0.8651	0.8845
tensile strength, MPa	4.0	12.1	14	9.0	20.2
strain to break, %	525	1260	960	1190	1060
yield stress, MPa					5
yield strain, %					66
recovery from 300% strain					
%set 1, 2, 3[h]	51	24	57, 30, n/a	52, 30, 26	54, 45, 26
%recovery 1, 2, 3[h]	83	92	81, 90, n/a	83, 90, 92	82, 85, 92

[a] Sample preparation and test conditions for ELPP-1 are different from those used for other samples. [b] See experimental for sample description. [c] Entry 6 from Table 4. [d] Entry 5 from Table 4. [e] Determined by high temperature GPC. [f] Determined by DSC. [g] Determined by ^{13}C NMR spectroscopy. [h] Three set and recovery values are based on (1) strain at return of stress to zero stress baseline on first cycle, (2) benchmarks measured on specimen, and (3) return to stress above baseline on second hysteresis cycle; this represents continuing time dependent recovery (1, 2, 3 are approximately 0, 30−60, 120 s from first cycle point).

monomer concentration, closely following the trends observed for **7**/MAO (Table 5).

Melting peaks observed in the DSC spectra of polypropylene samples generated with Cp*(2-PhInd)$ZrCl_2$ **8**/MAO were narrower than for samples of ELPP-7 (Figure 3). The enthalpies of fusion increased, and melting peaks shifted toward higher temperatures with increasing isotactic pentad content (Table 5). However, while the highest melting peaks for samples generated with (2-PhInd)$_2ZrCl_2$ **7**/MAO were observed at 130−150 °C, in the case of ELPP-8 all melting occurred below 105 °C (Table 5, Figure 3). The IR ratios, a measure of the isotactic helix content,[33] were consistently lower for samples of ELPP-8 than for samples of ELPP-7 with comparable % *mmmm* (Table 5). Furthermore, in contrast to ELPP-7, which could be fractionated into ether soluble, heptane soluble, and heptane insoluble fractions,[14,16,17] the sample of ELPP-8 with [*mmmm*] = 36% (entry 5 in Table 5) was found to be completely soluble in boiling ether.

Tensile stress/strain and recovery properties of ELPP-8 were found to be in the general range reported for other elastomeric polypropylenes (Table 6, Figure 4).[7−10,12] Lower M_w ELPP-8 (entry 6 in Table 4, ELPP-8−6, M_w = 124 000) exhibited high elongation to break (>1000%), good tensile strength (9 MPa), and high recovery (83−92%, within a few minutes after releasing stress). Higher M_w ELPP-8 (entry 5 in Table 4, ELPP-8-5, M_w = 455 000) exhibited higher strength (20.2 MPa), with elongation to break and recovery/set similar to those for the lower M_w sample. The density of molded ELPP-8-5 indicated higher crystallinity than in the case of ELPP-8-6. Consistent with higher density and crystallinity, ELPP-8-5 exhibited a small yield maximum at 66% strain in tensile deformation, and higher initial modulus than ELPP-8−6 (24 MPa vs 9.8 MPa) (Figure 4). ELPP-8 appeared to be at least equivalent in recovery and tensile properties to ELPP-1 of about the same molecular weight. However, the test methods in the case of the two polymers were not identical, and this comparison should be considered approximate. Recovery properties of ELPP-8-6 were similar to those of a higher molecular weight sample of ELPP-7.

Discussion

Zirconocene Structure. X-ray crystallographic analysis of complexes **8** and **9** reveals Zr−centroid bond lengths and angles

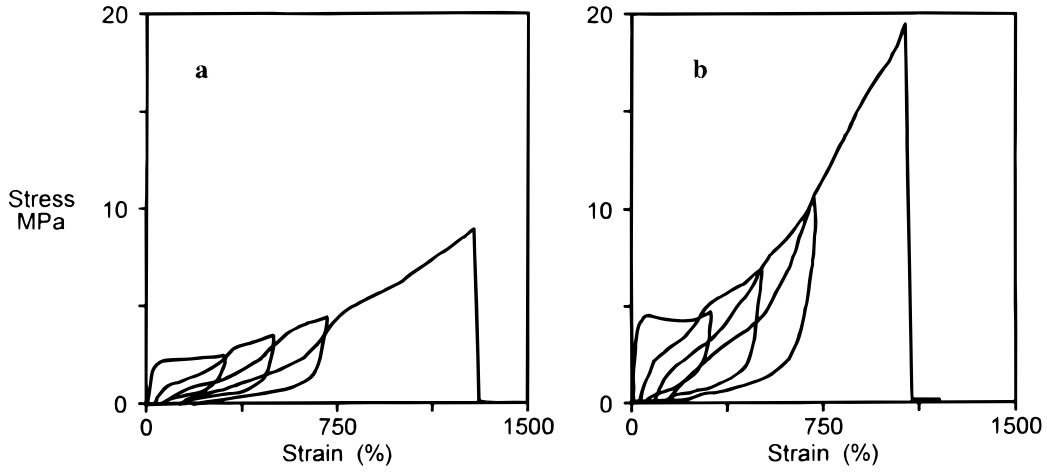

Figure 4. Hysteresis recovery test on polypropylene samples generated with Cp*(2-PhInd)$ZrCl_2$ **8**/MAO, elongation 300%, 500%, 700% and to break: (a) for sample description see Table 4 entry 6, (b) for sample description see Table 4 entry 5.

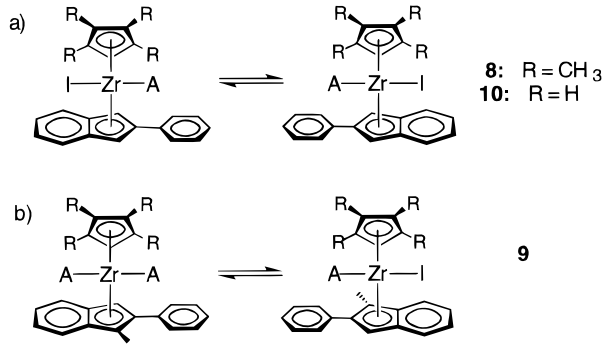

Figure 5. Possible rotamers of complexes **8**, **10** (a) and **9** (b).

which are similar to those observed for unbridged bis(2-arylindenyl) complexes.[14,18,25] Strong steric repulsion between 1-methyl and 2-phenyl substituents significantly increases the dihedral angle between the planes of the phenyl and the indenyl rings in complex **9**.[25]

^1H and ^{13}C NMR spectra are consistent with C_s-symmetry for Cp*(2-PhInd)$ZrCl_2$ **8** and Cp(2-PhInd)$ZrCl_2$ **10** and C_1-symmetry for Cp*(1-Me-2-PhInd)$ZrCl_2$ **9**. Similar to complex (2-PhInd)$_2ZrCl_2$ **7**, all three mixed-ring complexes appear to be fluxional on the NMR time scale at room temperature. However, the ligand rotation in the actual active species derived from complexes **7**−**10** is likely to be influenced by the interaction with the growing polymer chain and/or MAO-counterion. Possible low energy conformations for the metallocene cations derived from complexes **8**−**10** are depicted in Figure 5.[36] Assuming that the preferred enantioface for propylene coordination is determined by the steric interaction of its methyl group with the ligand substituents in the proximity of the catalyst active site,[37,38] the two coordination sites of each rotamer have been assigned as either aspecific (A) or isospecific (I). The symmetry of the rotamers of **8**/MAO and **10**/MAO depicted in Figure 5 is analogous to the symmetry of Chien's and Collins' bridged catalysts (**1**-**6**/MAO, Scheme 1).

Polymerization Behavior. Productivities and polymer molecular weights observed for catalysts **8**- and **9**/MAO in ethylene polymerization are very similar to those for **7**/MAO. However, the replacement of one of the 2-phenylindenyl ligands in zirconocene **7** with a cyclopentadienyl ligand (catalyst **10**) leads to a significant increase in ethylene polymerization productivity suggesting that the electronic nature of the Cp ligand, which lacks electron-donating substituents such as methyl groups in Cp* or a phenyl group in 2-phenylindenyl, must be a favorable factor in ethylene polymerization. Steric factors appear to be more important in propylene polymerization since the productivities follow a steric trend: Cp*(1-Me-2-PhInd)$ZrCl_2$ ≪ Cp*(2-PhInd)$ZrCl_2$ < (2-PhInd)$_2ZrCl_2$ < Cp(2-PhInd)$ZrCl_2$.

Lower molecular weights of polymers generated by Cp(2-PhInd)$ZrCl_2$ **10**/MAO as compared to those observed for (2-PhInd)$_2ZrCl_2$ **7**/MAO suggest a faster rate of chain termination with the former catalyst. It has been demonstrated before that the presence of substituents in position 2 (α to the bridge) in *ansa*-zirconocene catalysts leads to the increase of polypropylene molecular weight presumably by sterically shutting down chain termination via β-H transfer to the coordinated monomer.[39−41] It is possible that the presence of a 2-substituent on only one of the ligands gives way to this chain-termination process in polymerization with **10**/MAO and lowers the polymer molecular weights.

The unusually broad molecular weight distribution in polypropylene generated with catalyst **9**/MAO suggests that the rate of interconversion of the two rotamers may be even slower than formation of a single polypropylene chain which leads to heterogeneity of the resulting polymer. Similarly, broad MWD were observed for polypropylenes generated with bis(1-methyl-2-phenylindenyl)zirconocenes.[25]

Only one of the coordination sites in two rotamers of Cp*-(1-Me-2-PhInd)$ZrCl_2$ **9** is isospecific (Figure 5). In agreement with this the isotactic pentad content in polypropylene generated

(34) Cheng, H. N.; Smith, D. A. *Macromolecules* **1986**, *19*, 2065−2072.
(35) Cheng, H. N.; Ewen, J. A. *Makromol. Chem.* **1989**, *190*, 1931−1943.
(36) The geometry of the low energy rotamers depicted in Figure 5 is supported by the ligand orientation in the crystal structures of **8** and **9** and by computer modeling results obtained for **8**/MAO by Eric Moore at Amoco.
(37) Brintzinger, H. H.; Fischer, D.; Muelhaupt, R.; Rieger, B.; Waymouth, R. M. *Angew. Chem., Int. Ed. Engl.* **1995**, *34*, 1143−1170.
(38) Corradini and co-workers suggest that the enantioselectivity of a propene insertion is determined by the orientation of the first C−C bond of the growing polymer chain which is imposed onto it by the ligand environment, see: Corradini, P.; Guerra, G. *Prog. Polym. Sci*. **1991**, *16*, 239−257. According to Corradini, the assignments of the site stereospecificity in both rotamers of **8** and **10** and one of the rotamers of **9** should be interchanged, but it does not change the overall specificity of the rotamer.
(39) Herrmann, W. A.; Rohrmann, J.; Herdtweck, E.; Spaleck, W.; Winter, A. *Angew. Chem., Int. Ed. Engl.* **1989**, *28*, 1511−1512.
(40) Roll, W.; Brintzinger, H. H.; Rieger, B.; Zolk, R. *Angew. Chem., Int. Ed. Engl.* **1990**, *29*, 279−280.
(41) Stehling, U.; Diebold, J.; Kirsten, R.; Roll, W.; Brintzinger, H. H.; Jungling, S.; Mulhaupt, R.; Langhauser, F. *Organometallics* **1994**, *13*, 964−970.

with this catalyst is low (% *mmmm* = 17). Despite the fact that complexes **8** and **10** have the same symmetry, the catalysts generated from these zirconocenes give polypropylene of different tacticities: polypropylene produced with **8**/MAO is isotactically enriched and elastomeric, while the polymer produced with **10**/MAO is essentially atactic and amorphous. The difference in propylene polymerization behavior of the latter two catalysts suggests the importance of the methyl groups on the Cp*-ligand for stereo-differentiation.

Polymer Properties. The mechanical properties of elastomeric polypropylenes prepared with Cp*(2-PhInd)$ZrCl_2$ **8**/MAO, measured at room temperature, appear to be similar to those previously measured for other metallocene-derived elastomeric polypropylenes ELPP-1 and ELPP-7. While comparisons are difficult due to the differences in testing methods and sample histories, the tensile strengths of these materials fall in a range of 4−20 MPa, with elongations of 500−1300% and elastic recoveries of 80−90%.[10,14] However, thermal analysis of these polymers reveals important differences. Polypropylenes produced from (2-PhInd)$_2ZrCl_2$ **7**/MAO exhibit very broad melting transitions with peak melting points of 130−150 °C. In contrast, polypropylenes produced from mixed-ring complex Cp*(2-PhInd)$ZrCl_2$ **8**/MAO as well as polymers from Chien's and Collins' *ansa*-metallocenes **1**−**6**/MAO all melt below 100 °C. Furthermore, IR indices for samples of ELPP-8 are lower than in the case of (2-PhInd)$_2ZrCl_2$-derived samples with similar % *mmmm*. The differences in polymer properties are also manifested in fractionation behavior: ELPP-7 can be separated into three fractions with different tacticities, while ELPP-8 and polypropylenes derived from Chien's and Collins' systems are entirely soluble in boiling ether. The complete solubility in ether, lower melting points, and IR indices of ELPP-8 suggest that the crystallizable isotactic sequences in this polymer are on the average shorter than in ELPP-7.

The similarities in the symmetry and ligand environment of Chien's catalyst **1**/MAO and Cp*(2-PhInd)$ZrCl_2$ **8**/MAO[42] and in the properties of the generated polymers suggest the possibility of a similar mechanism of stereoblock formation with these systems that is apparently distinct from that of (2-Phind)-$ZrCl_2$ **7**/MAO. Two different propagation models have been proposed to explain the microstructure of polypropylene produced by Chien's and Collins catalysts: the "two-state" model depicted in Scheme 1 and the "random" model in which the monomer insertion takes place competitively at the two inequivalent coordination sites.[13] The two-state model of Coleman and Fox predicts a concentration dependence on the stereospecificity of the polymerization reaction.[11] The data are not clear concerning the stereospecificity of Chien's catalyst with monomer concentration; Collins reports a decrease in stereospecificity with increasing monomer concentration.[12] For **8**/MAO we see a clear increase in stereospecificity with increasing propylene pressure which favors the "two-state" mechanism for this catalyst.[11] Note that the two "states" for this catalyst cannot be the rotameric forms (as proposed for **7**) since these two forms are enantiomeric and would thus have similar kinetic behavior. The other possibility is that the aspecific and isospecific states are those where the polymer chain occupies diastereotopic coordination sites. This model assumes that if the polymer chain migrates with every monomer insertion, that the rate of "back-skipping" of the chain[43] is only slightly faster than that of monomer insertion in order to create runs of isotactic stereosequences. This "two-state" mechanism might then also account for the broad molecular weight distributions (MWD = 3.2−6.5) observed for polypropylenes generated with **8**/MAO if the two reactive sites are predisposed to generate polymers of different molecular weights.[19,44]

Conclusions

The order of ethylene polymerization productivities (Cp*(1-Me2-PhInd)$ZrCl_2$ ≈ Cp*(2-PhInd)$ZrCl_2$ ≈ (2-PhInd)$_2ZrCl_2$ < Cp(2-PhInd)$ZrCl_2$) suggested that the lower electron donating ability of a Cp ligand, as compared to Cp* and 2-phenylindenyl, favors the catalyst productivity. In propylene polymerization the steric factors appear to be more important in determining the order of catalyst productivities (Cp*(1-Me-2-PhInd)$ZrCl_2$ ≪ Cp*(2-PhInd)$ZrCl_2$ < (2-PhInd)$_2ZrCl_2$ < Cp(2-PhInd)$ZrCl_2$).

Catalyst Cp*(2-PhInd)$ZrCl_2$ **8**/MAO is the only one of the three mixed-ring catalysts capable of producing elastomeric polypropylene. Mechanical properties of ELPP-8 fall into the typical range for metallocene-derived polypropylene elastomers. However, DSC, IR and fractionation tests reveal important differences between Cp*(2-PhInd)$ZrCl_2$- and (2-PhInd)$_2ZrCl_2$-derived polypropylenes and suggest that isotactic blocks in the former polymers are on the average shorter. The geometry of **8** and properties of polypropylene generated with **8**/MAO are similar to those reported for Chien's catalyst **1**/MAO, which indicates a possibility of a common polymerization mechanism for the two catalysts.

Acknowledgment. We gratefully acknowledge Amoco and the NSF (CHE-9615699) for financial support. We thank Dr. Christopher Tagge and Dr. Eric Moore for helpful discussions and Amoco for carrying out high-temperature GPC analyses. R.M.W. is the recipient of the Waterman Award for which he is grateful. R.K. is the recipient of the McBain Fellowship for which she is grateful.

Supporting Information Available: Complete description of the X-ray structure determination of complexes **8** and **9**, including atomic coordinates, anisotropic thermal coefficients, and bond lengths and angles and listing of ^{13}C NMR pentad distributions for representative samples (24 pages). See any current masthead page for ordering and Web access instructions.

JA973414+

(42) Both in **1**/MAO and **8**/MAO the bulky methyl substituents on the cyclopentadienyl ligand are in close proximity to the catalyst active sites. In the case of unsubstituted Cp-ligand (**2**-**6**/MAO) the active center environment is more open.

(43) Guerra, G.; Cavallo, L.; Moskardi, G.; Vacatello, M.; Corradini, P. *Macromolecules* **1996**, *29*, 4834−4845.

(44) Coleman, B. D.; Fox, T. G. *J. Am. Chem. Soc.* **1963**, *85*, 1241−1244